AUTEX Research Journal, Vol. 16, No 2, June 2016, DOI: 10.1515/aut-2015-0036 © AUTEX

DE GRUYTER OPEN

INVESTIGATION OF CIRCULAR WOVEN COMPOSITE PREFORMS FOR COMPOSITE PIPES

Hooman Amid[1*], Ali Asghar Asgharian Jeddi[2], Manouchehr Salehi[3], Hadi Dabiryan[2] and Reza Pejman[3]

[1]College of Textiles, North Carolina State University, Raleigh, NC, USA, 1000 Main Campus Dr. Raleigh, NC 27695;
[2]Department of Textile Engineering, Amirkabir University of Technology, Tehran, Iran, 424 Hafez Avenue, PO Box 15875–4413, Tehran, Iran;
[3]Department of Mechanical Engineering, Amirkabir University of Technology, Tehran, Iran, 424 Hafez Avenue, PO Box 15875–4413, Tehran, Iran;
[*]Corresponding author E-mail: hamid@ncsu.edu

Abstract:

The main traditional technique for commercial manufacturing of composite pipes is filament winding in which the winding angle and the discontinuity of the structure (caused by starting and ending points of the winding process) are two important matters of concern. In the present study, circular woven fabric with its orthogonal net-shaped continuous structure was produced from polyester yarns. Fabric was wet with epoxy and hand lay-up was used to manufacture the composite pipes. Composite pipes were subjected to internal hydrostatic pressure and their burst strength was recorded. In addition, tensile strength of flat laminas was assessed in the warp and weft directions. We estimated and analysed the failure strength of composite pipes using Tresca's failure criterion and Finite Element (FE) modeling. The experimental burst strength was almost 23% more than the FE model and 77% more than the theoretical estimate.

Keywords:

Composite pipes; burst strength; finite element analysis (FEA); circular woven fabric; hand lay-up.

1. Introduction

Steel pipes have been used in oil/gas transportation industry and their corrosion has been the main driver for finding a substitute for them. Composite pipes have been introduced to this industry to overcome the corrosion and decrease the costs of transporting and installing the pipes. In addition, composite pipes offer acceptable elastic modulus, high strength-to-weight ratio, low density, high resistance to chemicals, higher flow capacities than concrete pipes due to the inherent smooth internal surface, and good thermal insulation. Their light weight reduces the cost of construction and transportation and their corrosion resistance reduces the cost of maintenance while lengthening their lifetime [1-3].

The most widespread commercial technique to manufacture composite pipes is filament winding in which the anisotropic properties of the pipes can be designed according to the winding angle [1]. Other parameters that should be considered when manufacturing filament wound composite (FWC) pipes are the angle-ply orientation, structure symmetry or asymmetry, number of layers, and fibre volume fraction [4, 5]. Different angle-plies result in differently applied hoop-to-axial stress ratios in each layer; this ratio should be 2:1 for all the layers within thin-walled FWC structures [6]. If the ratio of outer diameter to inner diameter is less than 1.1 the tube is considered as thin-walled, otherwise it is called thick-walled. Thin-walled structures have better strength-to-weight ratio and thick-walled structures have higher stiffness [3, 5]. The optimum winding angle is 55° when the ratio of applied hoop-to-axial stress is 2:1, and in case of no axial stress, the optimum angle is 75° [7]. The winding angle is an important design parameter [4, 8, 9]. Rosenow [10] has reviewed and concluded that the winding angle has pronounced effects on deformation, weeping and failure mechanisms of FWC pipes and vessels. To do the mechanical analyses, different test methods [11-13] to simulate diverse conditions and failure mechanisms [5, 14, 15] are available in the literature [13, 16-18].

Handling and installation of FWC structures could result in initial defects and cracks. Therefore, many studies have investigated the effect of initial defects and cracks on the failure and fatigue behaviour of FWC structures [2, 4, 19, 20]. It was concluded that the stress field and crack growth behaviour depend on crack shape, size, inclination and pipe dimensions. However, it should be stressed that the angle (inclination) of the crack is found to play the most prominent role.

Braided and woven structures such as plain woven roving, woven fibreglass fabrics, carbon fabric plies, etc. have been wound onto mandrels to form FWC pipes and fibre-reinforced steel tubes [16, 20-25]. Plain weave fabric has the same architecture as the circular woven fabric does, except for the discontinuity of the preform owing to the starting and ending points of wrapping. Sharma et al [26] have developed an algorithm to predict the drape behaviour and alignment of constituent fibres in circular woven fabric hoses. They have found that alignment of the constituent fibres, and fabric extensibility and buckling behaviour directly influences the structural homogeneity and mechanical properties in the final composite product [26]. It is reported that crack initiation (crack origin) happens from the inner surface, normal to the hoop stress, at the starting point of winding. The crack then propagates through the thickness and pipe bursts at the point that winding ends [13, 21].

It was hypothesized that stress concentration occurs at these starting and ending points since the filament (or woven fabric preform) is discontinuous. Having reviewed the literature, we found it worthwhile investigating the effect of orthogonal (net-shaped), seamless (continuous) structure of circular woven fabric on the mechanical properties of composite pipes. It should be stressed that the innovative part of this research is the application of continuous (seamless) circular preform for FWC pipes. This unique structure was believed to have profound influences on the reduction of stress amplification occurring on the outermost layer of the pipe. The main idea was hypothesised based on two facts: (1) in circular woven preforms the weft yarns position/lay perpendicular to the applied circumferential stress and would present their highest performance; (2) seamless and continuous structure would eliminate the stress concentration on starting-ending points.

2. Materials and Specimen Preparation

First, the right choice of yarn was made depending on its processability on the loom and then the fabric was produced. The circular fabric was used to make the tubular composites and some fabric samples were cut into flat single-layer specimens for tensile tests in both warp and weft directions. Flat specimens were later wet-laid into composite laminas. Testing of the flat composite laminas was required for the theoretical estimation and FE analysis of the mechanical properties of pipes.

2.1. Yarn and Fabric

According to the weaving possibilities on the available shuttle loom, polyester yarn was weavable and it was used for both warp, and weft yarn sets. At first, however, we tried to weave E-glass and carbon fibres that are typical fibres for composite applications. Glass and carbon fibres were found not to be weavable in the current state of the loom because the yarns tended to fall off the quill upon the beat of the picker stick, which its impact was not adjustable. Moreover, because of the high level of impact, induced by the picker's beat, brittle glass fibres tended to break. Table 1 demonstrates the physical and mechanical properties of the polyester yarn.

The yarn tensile test was performed according to ASTM D2256 and all the tensile tests on yarns, fabrics, and composite laminas were conducted on an INSTRON CRE testing machine. All of the presented values are from the average of five specimens per sample. For the yarn tensile tests, gauge length was 250 mm and the strain rate was 300 mm/min.

The circular fabric was produced by a Picanol shuttle loom. It is worthy of attention that circular structures can only be manufactured by shuttle looms and in order to do that the loom should be set to weave double cloth fabric structure. In shuttleless looms, the weft yarn is cut upon its arrival on each side of the machine to form a selvage, whereas in shuttle looms, the weft yarn follows a continuous path through the fabric's width. Adjusting the shedding system of shuttle loom, a circular woven fabric was produced by movement of weft yarn in two separate sheds. Based on the diameter of the tube, each quill can carry a single weft yarn meters along the fabric, resulting in the continuous seamless structure in the circular fabric. The weave was plain and physical and mechanical properties of the circular woven fabric are presented in Table 2.

The tensile tests were completed in accordance to BS 2576, with the specimen width, gauge length and strain rate being 50 mm, 250 mm and 100 mm/min, respectively.

Figure 1 shows the circular fabric after cutting in both warp and weft directions.

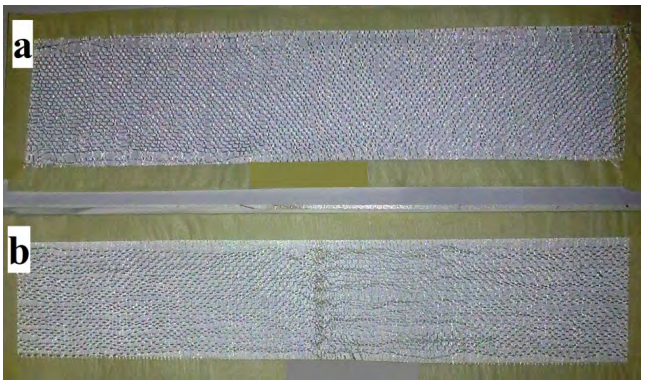

Figure 1. Circular woven fabric after cutting, a: warp direction, b: weft direction

Table 1. Physical and mechanical properties of polyester yarn (used for warp and weft yarn sets)

Linear density (tex)	Density (g/cm^3)	Twist per meter (TPM)	Tenacity (cN/tex)	Extension at failure (%)	Initial modulus (cN/tex)
69.5	1.38	650	30.7	12.03	245.86

Table 2. Physical and mechanical properties of the tubular woven fabric

Fabric density		Fabric weight per unit area (g/m^2)	Breaking force (N)		Extension at failure (%)	
Ends/cm	Picks/cm		Warp	Weft	Warp	Weft
5.9	7.1	197.5	483.41 (9.62)*	547.67 (4.75)	13.47 (2.49)	14.09 (5.61)
* Values in parenthesis indicate CV%.						

2.2. Flat Composite Laminas and Composite Pipes

To calculate the theoretical values for the internal hydrostatic pressure of composite pipes the tensile properties of flat composite laminas were investigated. It should be taken into consideration that warp yarns are the reinforcing component in the axial direction of the pipe and the weft yarns reinforce the pipe in the radial (hoop) direction.

After cutting the fabric into flat specimens, they were wet using epoxy resin and subsequently hand laid-up. The Epoxy resin system consists of Araldite LY5052, with the density of 1.17 g/cm^3, and Aradur 5052, with the density of 0.94 g/cm^3, as the hardener (curing agent/initiator). Based on the mix ratio, the density of the mixed matrix was 1.106 g/cm^3; mix ratio is defined by AHEW (Amine Hydrogen Equivalent Weight), which was 38 (g/eq), and the resin EEW (Epoxy Equivalent Weight).

After wet-laying the fabric, a pressure of about 9 kPa was applied on the layup assembly, shown in Figure 2, to remove the excess resin. Vaseline was applied on the plastic separating films as the release agent to be able to take off the laminas easier. The pressure was provided by putting some free weights on the layup assembly and it was kept there for the duration of the curing (24 hours at RT). Subsequently, the specimens were postcured for 15 hours at 50ºC.

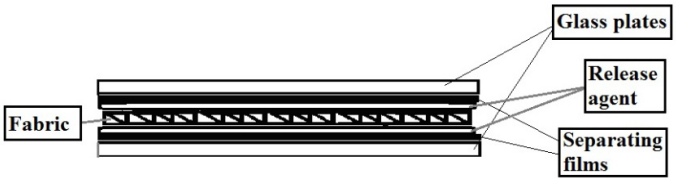

Figure 2. The set used for hand lay-up process of flat composite laminas

The physical properties of the flat composite laminas are presented in Table 3. It should be mentioned that these properties are same in both weft and warp directions because the fabric was first wet-laid and then cut into standard size of specimens in specified directions.

The fibre and matrix volume fractions were measured and calculated based on ASTM D3171. The thickness was measured at five different places (from the edges to the middle) of the laminas.

To produce the composite pipes, the circular woven structure was laid-up onto a cylindrical polyethylene mandrel that had been machined to fit the diameter of the circular fabric. Then the resin was applied to the preform using a stick to prevent the rearrangement of the yarns. This was done by pouring the resin on the preform and distributing it by a stick, because using a brush could rearrange the structure that should be avoided. Finally, a wide plastic tape was wrapped around the impregnated preform on the mandrel and specific amount of weight was attached to the wrapped tape. This was done with the consideration that the same pressure (9 kPa - as for the flat specimens) would be applied on the composite pipe to have the same thickness as for the flat specimens. The amount of resin applied on the preform was in accordance to the fibre volume fraction of flat laminas. After solidification and curing (24 hours at RT), the pipes were demoulded and postcured (15 hr at 50ºC). It should be stressed that the impregnation, lay-up and consolidation processes were done in such a manner to prevent any rearrangement of the constituent yarns. The mandrel that was used to hand-layup the composite pipe and the final manufactured composite pipes are shown in Figures 3 and 4, respectively.

Figure 3. The mandrel used for producing composite pipe (while wetting the preform)

Figure 4. Composite pipes

Table 3. Physical properties of the flat composite laminas

Weight per unit area (g/m^2)	Thickness (mm)	Fibre volume fraction (%)	Matrix volume fraction (%)	Density (g/cm^3)
1058	0.865 (±0.025)	10.14	89.86	1.223

Table 4. Physical properties of the composite pipes

Weight per unit area (g/m^2)	Wall thickness (mm)	Fibre volume fraction (%)	Inner diameter and pipe length (mm)	Density of lamina (g/cm^3)
1045	0.855 (±0.035)	10.19	101 and 300	1.219

The physical properties of composite pipes are demonstrated in Table 4.

3. Tensile and Hydrostatic Pressure Tests

The tensile tests on flat composite laminas were performed by INSTRON CRE tester according to ASTM D3039. The gauge length and sample width were 250 mm and 25 mm, respectively, and the strain rate was 10 mm/min.

Testing the composite pipes was challenging because of the low thickness (0.855 mm) of pipes and the resultant low stiffness and rigidity. Because of the mentioned low stiffness, standard test methods, such as out-of-plane or in-plane bending test, ring test etc., could not be applied. Thus, two polyethylene caps were machined to fit the diameter of the pipes, one of which with an axial hole for the oil flow in the hydrostatic test. Figure 5 demonstrates the dimensions of the composite pipes and the caps.

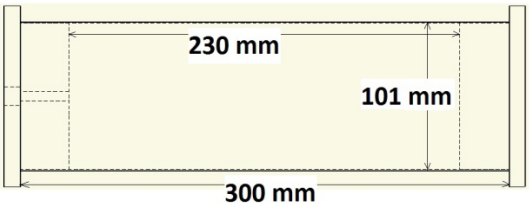

Figure 5. Dimensions of the produced composite pipes (including the caps)

Two ring clamps were used to ensure that the caps would not move away during the pressure test. Plastic bags were used to prevent spilling the oil after the pipes burst. A hydraulic jack was used to perform the hydrostatic pressure test and the burst time for all composite pipes was 30 seconds ± 5. The setup that was used to perform the hydrostatic pressure test is shown in Figure 6.

A gap of 10 mm was kept between the caps edges and pipe ends. This was to ensure that the pipes could extend axially during the test and there is no restriction on axial strain. Furthermore, the ratio of outer diameter to inner diameter of pipes was less than 1.1 (101.865/101 = 1.008) so that the pipe was considered thin-walled.

4. Theoretical Approach and Finite Element Modeling

4.1. Theoretical Approach

The goal of the theoretical section of this work was to evaluate the experimental results and any discrepancies between the theoretical and experimental results. Therefore, different failure criteria were considered including the ones for orthotropic composite materials (Maximum Stress, Maximum Strain, Tsai-Wu, Tsai-Hill, etc.) and the ones for isotropic materials (Maximum Distortion Energy (Von Mises) and Maximum Shear Stress (Tresca)). Thin-walled tubes subjected to internal pressure, experience two stresses, that is, axial stress and hoop (circumferential) stress. Therefore, simpler criteria, either Tresca or Von Mises were applicable. The axial stress was not present in our case since the end caps were not fixed, so both criteria would yield the same results. To investigate the

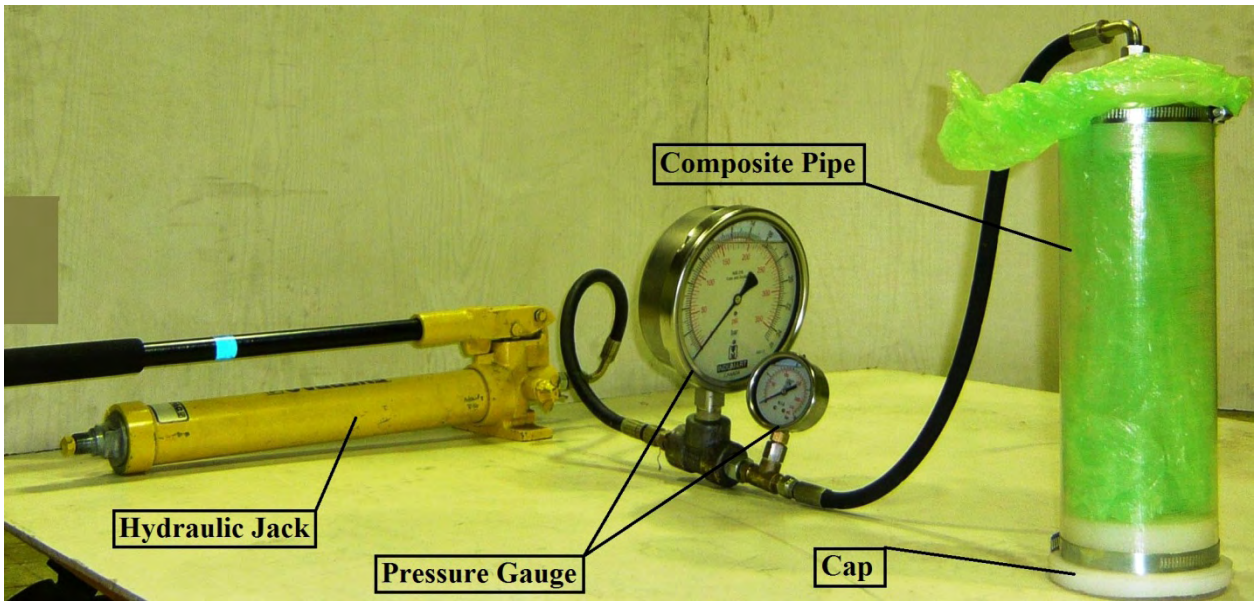

Figure 6. The set used for hydrostatic pressure test

performance of the orthogonal net-shaped preform structure in the hoop direction and estimate the theoretical composite pipe burst strength, Tresca failure criterion was applied. Equation (1) shows the Tresca's failure criterion [27]:

$$|\sigma_a - \sigma_b| \leq \sigma_y \quad (1)$$

where σ_y is the yield stress, σ_a is the maximum principal stress and σ_b is the minimum principal stress. In the case of thin-walled pipes, the principal stresses are hoop (circumferential) (σ_h) and axial (longitudinal) stress (σ_l). Since the hoop direction has been studied, yield stress (σ_y) corresponds to the failure stress of flat composite laminas in the weft direction.

On the other hand, based on Hook's Law for thin-walled cylinders [27], equations (2) and (3) are presented as follows:

$$\sigma_l = {}^{pr}/_{2t} \quad (2)$$

$$\sigma_h = {}^{pr}/_{t} \quad (3)$$

where '*p*' is the applied pressure, '*r*' is the radius of the tube, and '*t*' is the thickness of the pipe. For thin-walled cylinders the radial stress is zero; so the maximum principal stress is the hoop (or circumferential) stress ($\sigma_a = \sigma_h$) and the minimum principal stress is the radial stress ($\sigma_b = \sigma_\theta = 0$). Since the two ends were free to move in our experiments, the axial stress was also zero. Substituting Equations 2 and 3 in Equation 1 result in Equation (4):

$$\begin{aligned} {}^{pr}/_{t} - 0 &\leq \sigma_y \\ {}^{pr}/_{t} &\leq \sigma_y \\ p &\leq \frac{t\sigma_y}{r} \end{aligned} \quad (4)$$

where 'p' is the estimated failure pressure of composite pipes in (kPa), 'σ_y is the tensile strength of the flat composite lamina in the weft direction in (kPa), 't' is the wall thickness in (mm) and 'r' is the inner radius of the pipe in (mm). It is notable that the burst strength of cast iron pipes can be calculated by Equation 4.

4.2. Finite Element Modeling

Polyester-Epoxy Plate Model Description

The polyester/epoxy plates were considered as rectangles with the dimensions of 317.3 mm × 230 mm in two various cases under tensile load (see Figure 7(a) & 7(b)). To mesh the model, four-nodded element with six degree of freedom at each node was used. The number of elements was more than 1500. Figure 7(c) shows the schematic representation of the mesh.

It was tested and verified that the modelling size and the mesh are insensitive to the far-field boundary. One edge of the plate was fixed and the other edge was under tension. The static analysis was carried out using ANSYS. Material properties are listed in Table 5 where E, G, and v are the Young's modulus, the Shear modulus, and the Poisson's ratio, respectively.

Polyester-Epoxy Pipe Model Description

The simulated sample of the present study, shown in Figure 8(a), consists of a polyester-epoxy pipe. Four-nodded element with six degree of freedom at each node was used to mesh the model. This element was well suited for linear, large rotation and/or large strain nonlinear applications. The number of elements was more than 3000. Thickness of this model was divided into five sections in radial direction. Each section has the thickness of 0.171 mm that alternatively has the direction of 90 degree or 0 degree. Figure 8(b) shows the schematic representation of the mesh.

It was tested and verified that the modeling size and the mesh are insensitive to the far-field boundary. One end of shell was

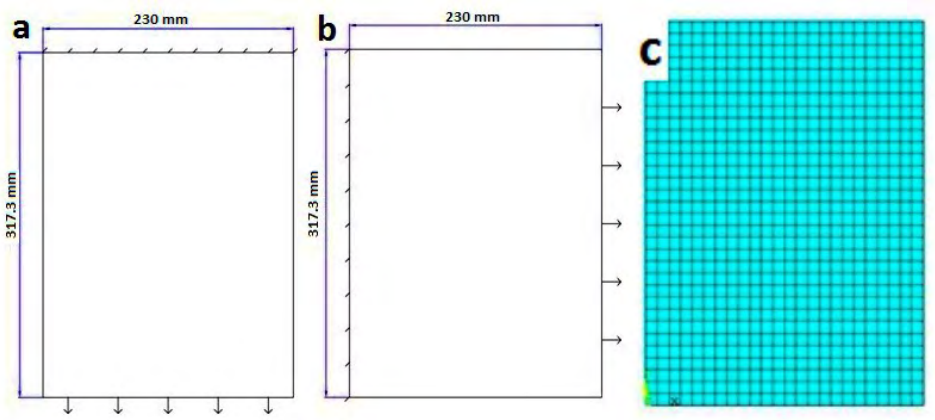

Figure 7. Model geometry and mesh schematic of the plate under tension, (a) warp dir., (b) weft dir., (c) mesh

Table 5. Material properties of components

Material	E_x (GPa)	E_y (GPa)	E_z (GPa)	v_{xy}	v_{yz}	v_{xz}	G_{xy} (GPa)	G_{yz} (GPa)	G_{xz} (GPa)	ρ (g/cm^3)
polyester/epoxy	0.531	0.667	1.853	0.35	0.11	0.094	0.309	0.300	0.307	1.223

fixed by roller boundary condition in the longitudinal direction. The static analysis was carried out using a commercial finite-element package.

5. Results and Discussions

5.1. Tensile and Hydrostatic Pressure Tests

Table 6 presents the results of tensile tests for flat composite laminas in both warp and weft directions.

The results of the hydrostatic pressure test for all specimens are presented in Table 7.

Inserting the values of tensile strength of the weft direction in Equation (4):

$$p \leq \frac{0.855 \times 21280}{50.5} = 360\ (kPa)$$

It was estimated that the burst strength of composite pipes was 360 kPa. The average burst pressure for the composite pipes was 638 kPa that is about 11 percent more than the theoretical estimate. The source of this difference can be attributed to the superior structural properties of orthogonal and continuous tubular woven preform. The fractured composite pipes are shown in Figure 9.

It can be seen that the fractures are initiated and propagated in the axial direction that verifies the fact that hoop stress

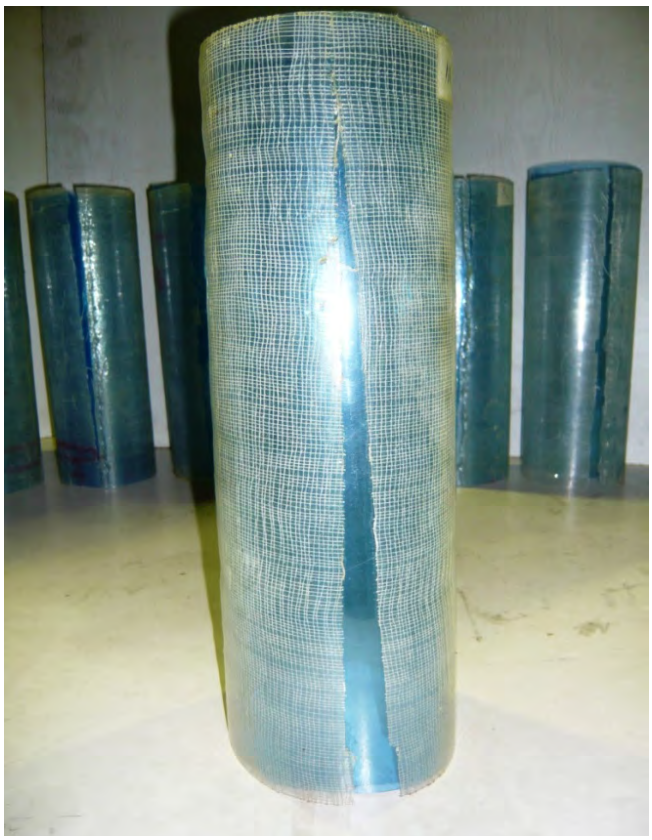

Figure 9. Tubular composite pipes after fracture (the blue transparent plastic sheet was put inside to be able to recognize the crack in the photo)

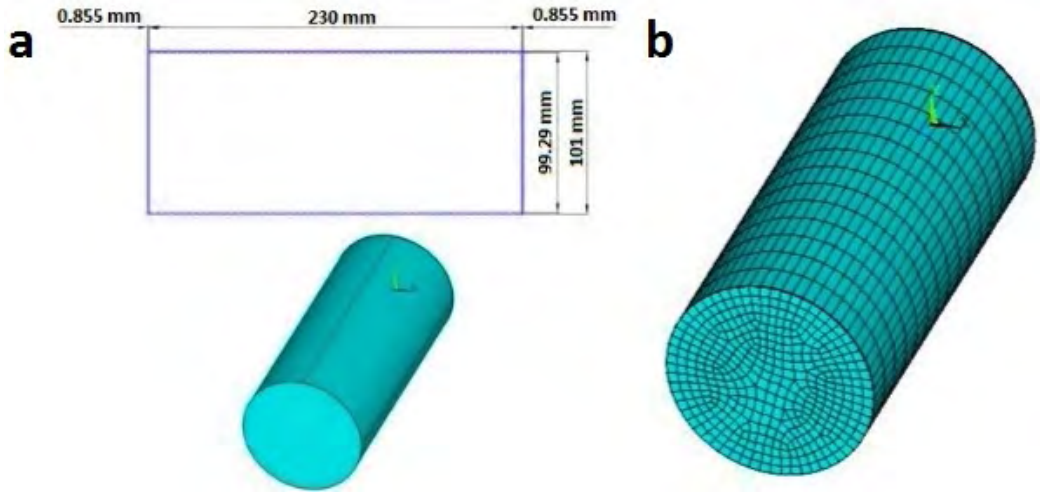

Figure 8. (a) Model geometry and (b) mesh schematic of close end shell

Table 6. Tensile properties of flat composite specimens

Test direction	Maximum load at failure (N)	Tensile strength (mPa)		Extension (%)	
		Mean	CV%	Mean	CV%
Warp	428.11	19.80	(11.01)	3.73	(8.79)
Weft	460.22	21.28	(14.93)	3.19	(6.21)

Table 7. Burst strength of tubular composite pipe specimens

Test specimens	1	2	3	4	5	Mean	CV%
Burst strength (kPa)	600	630	870	520	570	638	21.3

was more than axial stress. Moreover, the axial fracture direction confirms the assumption we made when adopting the theoretical approach.

Because of the single-layer structure of the produced tubular composite pipe, and since there is no FWC pipe with such a single-layer structure, we have compared the value of the burst strength to that of a typical cast iron pipe. Having known the tensile strength of cast iron [27], the burst strength of such a pipe is calculated by Equation (4). To compare the values of burst strength of cast iron pipes and tubular composite pipes, specific burst strengths (or strength-to-weight ratio) have been compared. This is the failure stress of the material divided by its density. The tensile strength and density of cast iron are 210 (mPa) and 7.64 (kg/m^3), respectively [27]. Thus, based on Equation (4), for pipe dimensions of this study, its specific burst strength would be 465.37 (N.m/kg). This value is calculated for the tubular composite pipe in the same manner and Table 8 shows the comparison between the theoretical value and specific strengths of composite pipes and cast iron pipes.

5.2. Finite Element Results

The FE and experimental results for both polyester/epoxy plate and pipe are compared in Table 9.

The composite plate was under tensile load in two different directions, and the composite pipe was under internal pressure. Internal pressure was varied from 70 kPa to 700 kPa and the maximum circumferential stress on the shell was recorded accurately. Figure 12 compares the finite element results of the variation of maximum circumferential stress under various internal pressures with theoretical results, calculated based on Equation 3. As shown in Figure 10, the burst pressure was estimated to be about 520 kPa by the finite element method.

It was hypothesised that the seamless (continuous) orthogonal net-shaped structure of the preform is the major reason for the difference between experimental burst strength of the composite pipe and both the FE model and the theoretical estimate. It was seen that the specific strength of tubular

Table 8. Comparison between theoretical and experimental values of burst strength and between specific burst strengths of cast iron and tubular composite pipes

Theoretical burst strength (kPa)	Experimental burst strength (kPa)	Specific burst strength of composite pipes (N.m/kg)	Specific burst strength of cast iron pipes (N.m /kg)
360	638	523.38	465.37
+77% difference (desired)		+ 12.5% difference (desired)	

Table 9. Experimental results vs. FE results (tensile and internal pressure tests)

Direction	Finite Element	Experimental	Percentage of difference
Warp tensile strength	21 mPa	19.80 mPa	-5.71%
Weft tensile strength	20.35 mPa	21.28 mPa	4.57%
Pipe burst strength	520 kPa	638 kPa	22.69%

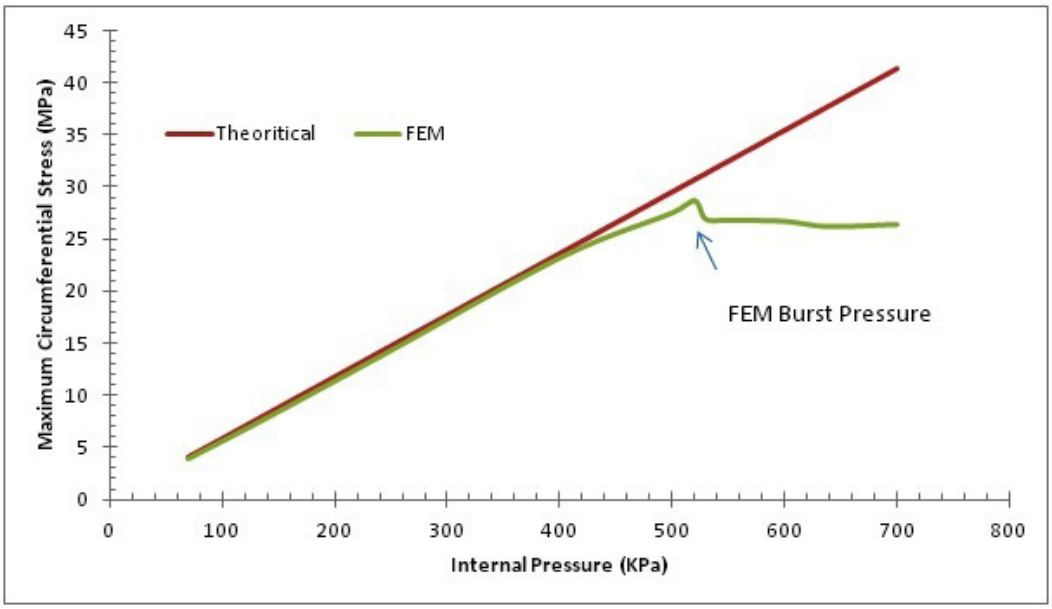

Figure 10. Maximum circumferential stress vs. internal pressure

composite pipes was 12.5% more than that of cast iron pipes that is quite promising about the structural applicability of tubular composite pipes in the field of composite pipes. Talking about this small difference, one should bear in mind that the reinforcement constituent in this research is a typical textile polyester yarn with tensile modulus of about one twentieth that of fibre glass which is typically used in this field. Therefore, the resultant burst strength is mainly governed by the structural superiority of tubular woven composite pipe over FWC structures. This is due to (a) the perpendicular alignment of weft yarns to the hoop stress and (b) continuous seamless structure. The weft yarns place in the hoop direction and the hoop stress acts perpendicularly to weft yarns; therefore, they can bear the tension more efficiently. On the other hand, it is clear that the absence of starting and ending points of winding in this structure makes it continuous and seamless. The continuity reduces the stress concentration and amplification in the first and last layers and yields a uniform stress distribution over the whole structure. Since having a single-layer FWC pipe was not achievable, we did not test/compare our composite pipe with FWC pipes.

6. Conclusions

Tubular woven fabrics were produced by a shuttle loom and then tubular composite pipes were produced by hand lay-up method. The pipes have net-shaped orthogonal, continuous structure that, in comparison to FWC structures, their weft yarns are perpendicular to the hoop force. In addition, there is no starting/ending point for winding which makes the structure continuous and seamless. Since the preform had an orthogonal structure, Tresca's failure criterion was adopted to estimate the theoretical values of burst strength. Performing hydrostatic pressure tests, the experimental burst strength was 77% more than the theoretical estimate. Since the structure is not comparable to that of FWC, it was compared to typical cast iron pipes with the same size; specific burst strength of the composite pipe was 12.5% more than that of cast iron pipe. To build confidence in our experimental results, we performed Finite Element analysis; it was found that the burst strength of tubular composite pipes was almost 23% more than the FE result. The superior burst strength was due to the continuous net-shaped structure of the composite pipe. The circular woven preform provides a seamless continuous reinforcement for composite pipes with no starting-ending point(s); this reduces stress amplification-concentration at those points. The perpendicular positioning of the weft yarns with respect to the applied hoop stress is the other advantage of such preform structure. Therefore, investigating the effect of different weft densities and fabrication techniques on the burst strength is the subject of future studies.

Acknowledgements

The authors thank Dr. Philip Bradford at North Carolina State University for useful discussions.

References

[1] Czel G., Czigany,T., (2012). Image processing assisted stress estimation method for ring compression tests of polymer composite pipes at large displacements. Journal of Composite Materials, 46(22), 2803-2809.

[2] Arikan H., (2010). Failure analysis of (+/- 55 degrees)(3) filament wound composite pipes with an inclined surface crack under static internal pressure. Composite Structures, 92(1), 182-187.

[3] Diniz Melo J. D.,Levy Neto,F.,Barros,G. d. A.,de Almeida Mesquita,F. N., (2011). Mechanical behavior of GRP pressure pipes with addition of quartz sand filler. Journal of Composite Materials, 45(6), 717-726.

[4] Sari M.,Karakuzu,R.,Deniz,M. E.,Icten,B. M., (2012). Residual failure pressures and fatigue life of filament-wound composite pipes subjected to lateral impact. Journal of Composite Materials, 46(15), 1787-1794.

[5] Onder A.,Sayman,O.,Dogan,T.,Tarakcioglu,N., (2009). Burst failure load of composite pressure vessels. Composite Structures, 89(1), 159-166.

[6] Xia M.,Takayanagi,H.,Kemmochi,K., (2001). Analysis of multi-layered filament-wound composite pipes under internal pressure. Composite Structures, 53(4), 483-491.

[7] Bakaiyan H.,Hosseini,H.,Ameri,E., (2009). Analysis of multi-layered filament-wound composite pipes under combined internal pressure and thermomechanical loading with thermal variations. Composite Structures, 88(4), 532-541.

[8] Frost S. R., Cervenka,A., (1994). Glass-fiber-reinforced epoxy matrix filament-wound pipes for use in the oil industry. Composites Manufacturing, 5(2), 73-81.

[9] Kruijer M. P.,Warnet,L. L.,Akkerman,R., (2006). Modelling of the viscoelastic behaviour of steel reinforced thermoplastic pipes. Composites Part A-Applied Science and Manufacturing, 37(2), 356-367.

[10] Rosenow M. W. K., (1984). Wind angle effects in glass fiber-reinforced polyester filament wound pipes. Composites, 15(2), 144-152.

[11] Kitching R., Hose,D. R., (1989). Laminated pipe bends of mixed wall construction subjected to an inplane bending moment. Journal of Strain Analysis for Engineering Design, 24(3), 127-138.

[12] Kitching R.,Myler,P.,Tan,A. L., (1988). Grp pipe bends subjected to out-of-plane flexure with and without pressure. Journal of Strain Analysis for Engineering Design, 23(4), 187-199.

[13] Hwang T.,Park,J.,Kim,H., (2012). Evaluation of fiber material properties in filament-wound composite pressure vessels. Composites Part A-Applied Science and Manufacturing, 43(9), 1467-1475.

[14] Samanci A.,Avci,A.,Tarakcioglu,N.,Sahin,O. S., (2008). Fatigue crack growth of filament wound GRP pipes with a surface crack under cyclic internal pressure. Journal of Materials Science, 43(16), 5569-5573.

[15] Samanci A.,Tarakcioglu,N.,Akdemir,A., (2012). Fatigue failure analysis of surface-cracked (+/- 45 degrees) (3) filament-wound GRP pipes under internal pressure. Journal of Composite Materials, 46(9), 1041-1050.

[16] Cabrera N. O.,Alcock,B.,Klompen,E. T. J.,Peijs,T., (2008). Filament winding of co-extruded polypropylene tapes for fully recyclable all-polypropylene composite products. Applied Composite Materials, 15(1), 27-45.

[17] Arellano M. T.,Crouzeix,L.,Douchin,B.,Collombet,F.,Hern andez Moreno,H., et al, (2010). Strain field measurement of filament-wound composites at +/- 55 degrees using digital image correlation: An approach for unit cells employing flat specimens. Composite Structures, 92(10), 2457-2464.

[18] Ellyin F.,Carroll,M.,Kujawski,D.,Chiu,A. S., (1997). The behavior of multidirectional filament wound fibreglass/ epoxy tubulars under biaxial loading. Composites Part A-Applied Science and Manufacturing, 28(9-10), 781-790.

[19] Baranger E.,Allix,O.,Blanchard,L., (2009). A computational strategy for the analysis of damage in composite pipes. Composites Science and Technology, 69(1), 88-92.

[20] Buarque E. N., d'Almeida,J. R. M., (2007). The effect of cylindrical defects on the tensile strength of glass fiber/ vinyl-ester matrix reinforced composite pipes. Composite Structures, 79(2), 270-279.

[21] Kitching R.,Hose,D. R.,Preistner,R.,Hashemizadeh,S. H., (1997). Fracture of glass-reinforced plastic pipes of mixed wall construction under pressure loading. Proceedings of the Institution of Mechanical Engineers Part E-Journal of Process Mechanical Engineering, 211(E4), 223-246.

[22] Yu H. N.,Kim,S. S.,Hwang,I. U.,Lee,D. G., (2008). Application of natural fiber reinforced composites to trenchless rehabilitation of underground pipes. Composite Structures, 86(1-3), 285-290.

[23] Fawzia S.,Al-Mahaidi,R.,Zhao,X. L.,Rizkalla,S., (2007). Strengthening of circular hollow steel tubular sections using high modulus CFRP sheets. Construction and Building Materials, 21(4), 839-845.

[24] Haedir J., Zhao,X., (2011). Design of short CFRP-reinforced steel tubular columns. Journal of Constructional Steel Research, 67(3), 497-509.

[25] Amid H.,Jeddi,A. A. A.,Salehi,M.,Dabiryan,H., (2011). Suitability of tubular woven fabric as the reinforcement of composite pipes. Proceedings of ATC-11Daegu, South Korea.

[26] Sharma S. B.,Potluri,P.,Atkinson,J.,Porat,I., (2001). Mapping of tubular woven composite preforms on to doubly-curved surfaces. Computer-Aided Design, 33(14), 1035-1048.

[27] Popov E. P., (1990).Engineering Mechanics of Solids. Prentice Hall (Englewood Cliffs, N.J.).